

# Humidity Sensitivity of Polypyrrole and Polypyrrole/SBA-15 Host–Guest Composite Materials

Wangchang Geng,<sup>1</sup> Xiaotian Li,<sup>1</sup> Nan Li,<sup>1</sup> Tong Zhang,<sup>2</sup> Wei Wang,<sup>1</sup> Shilun Qiu<sup>3</sup>

<sup>1</sup>Department of Material Science and Engineering, Jilin University, Changchun 130012, People's Republic of China

<sup>2</sup>Department of Electronic Engineering, Jilin University, Changchun 130012, People's Republic of China

<sup>3</sup>Department of Chemistry and State Key Laboratory of Inorganic Synthesis and Preparative Chemistry, Jilin University, Changchun 130012, People's Republic of China

Received 2 March 2006; accepted 15 May 2006

DOI 10.1002/app.24769

Published online in Wiley InterScience (www.interscience.wiley.com).

**ABSTRACT:** Polypyrrole (PPY) and PPY/SBA-15 host-guest composite materials have been prepared using chemical synthesis route and characterized by XRD, IR, N<sub>2</sub> adsorption-desorption isotherms, and SEM. The humidity sensitive properties (HSP) of this kind of materials have been studied by analyzing the variation curve of impedance as a function of relative humidity. It was found

that the PPY/SBA-15 host-guest composites materials exhibit better HSP than that of the corresponding pure PPY. © 2006 Wiley Periodicals, Inc. *J Appl Polym Sci* 102: 3301–3305, 2006

**Key words:** humidity sensitivity; polypyrrole; SBA-15; host-guest composite materials; conducting polymer

## INTRODUCTION

Humidity sensors have been widely used in the field of environment detection or monitoring.<sup>1–4</sup> Besides these, humidity sensors play an important role in libraries, museums, weather report, and food storages. It is important to exploit novel humidity sensitive materials for the development of the humidity sensors. In recent years, many efforts have been made to fabricate the proper polymers for humidity sensors.<sup>5–10</sup> Compared with the other conducting polymers, polypyrrole has relative high conductivity and environmental stability. So it is expected to have the potential application values in humidity sensors. Some works have been made to study the humidity sensitive properties (HSP) of the materials based on polypyrrole. However, as far as we know, the researches of the HSP of PPY/SBA-15 have not been reported.

In our work, we obtained the host-guest composite material PPY/SBA-15 using chemical method by encapsulating the polypyrrole (PPY) into the mesoporous silica SBA-15. Its HSP were studied using a ZL-5 model LCR analyzer. We found that PPY/SBA-15

host-guest composite material exhibit better HSP than the corresponding pure PPY.

## EXPERIMENTAL

### Materials

A hydrated ferric chloride (FeCl<sub>3</sub>·6H<sub>2</sub>O) was used without any purification as an oxidant for the chemical polymerization of pyrrole. Pyrrole was distilled under reduced pressure before use. Mesoporous silica SBA-15 was prepared in our laboratory according to the method reported by Zhao et al.<sup>11,12</sup> Anhydrous ethanol was used as solvents for the polypyrrole (PPY) synthesis.

### Preparation of SBA-15

Block copolymer surfactant P123 (EO<sub>20</sub>PO<sub>70</sub>EO<sub>20</sub>; 2.4 g) was mixed with 75 mL of distilled water under stirring. Subsequently, 11 mL of concentrated HCl (37.5%) was added. After stirring for 30 min, 5.1 mL of tetraethoxysilane was added dropwise under vigorous stirring at 45°C for 4 h. Then the mixture was transferred into stainless reactive kettle, and crystallized at 100°C for 24 h. The product was filtered and washed with distilled water, and the surfactant was removed by heat treatment in air at 550°C.

### Growth of PPY

PPY was obtained by chemical synthesis. The process is described as follows: 3.4 mL of pyrrole was dissolved in 25 mL of ethanol, and stirred for 10 min.

Correspondence to: X. Li (xiaotianli@jlu.edu.cn) or S. Qiu (squi@mail.jlu.edu.cn).

Contract grant sponsor: National Science Foundation; contract grant number: 20151001.

Contract grant sponsor: Natural Science Foundation of Jilin Province; contract grant number: 20040505.

Twenty milliliter of  $\text{FeCl}_3 \cdot 6\text{H}_2\text{O}$  ethanol solution ( $0.36 \text{ mol L}^{-1}$ ) was added dropwise to the ethanol solution of pyrrole. Instantaneously, a black colored precipitate could be observed. The mixed solution was magnetic stirred for 4 h at room temperature. The resultant solution was filtered and washed three times with ethanol, then dried in a vacuum box overnight.

### Growth of PPY/SBA-15 composites

The calcined SBA-15 was vacuumed to 10 Pa at 573 K for 24 h to remove air and water in the channel. The monomer pyrrole was adsorbed into the pores of SBA-15 through vapor at room temperature. The adsorption process was lasted for 24 h to improve the pyrrole level in the channel of SBA-15. The pyrrole-containing SBA-15 was immersed in the ethanol solution of  $\text{FeCl}_3 \cdot 6\text{H}_2\text{O}$  at room temperature under magnetic stirring for 24 h. Finally, the product was washed with ethanol and dried under vacuum.

### Methods of characterization

The X-ray power diffraction (XRD) patterns were collected on a Siemens D-5005 diffractometer (Siemens AG, Karlsruhe, Germany) using  $\text{Cu-K}\alpha$  radiation at 40 kV and 30 mA. The wide angle XRD patterns were recorded in the  $2\theta$  range of  $10\text{--}40^\circ$ , at a scanning speed of  $0.5^\circ \text{ min}^{-1}$ . The low angle XRD patterns were scanned from  $0.5^\circ$  to  $4.0^\circ$  at a scanning rate of  $1^\circ \text{ min}^{-1}$ .  $\text{N}_2$  adsorption–desorption isotherms were measured at 77 K on a Micromeritics ASAP 2010m instrument (Micromeritics Instrument Corp., Norcross, GA). Infrared spectra were taken on a Perkin–Elmer series with a resolution of  $4 \text{ cm}^{-1}$ . The morphology of products was characterized by a JEOL JSM-6700F field emission scanning electron microscope (SEM). The variation curve of impedance as a function of relative humidity was measured on a ZL-5 model LCR analyzer at room temperature, 1 kHz, and 1.0 V. The pure PPY and PPY/SBA-15 power materials was screen printed on a ceramic plate ( $1 \times 0.5 \text{ cm}^2$ ) in which the interdigitated gold electrodes was printed and heated.

## RESULTS AND DISCUSSION

### X-ray diffraction

The XRD patterns of SBA-15 and PPY/SBA-15 were shown in Figure 1. We could see that the three peaks, which were attributed to (100), (110), and (200) of SBA-15 [Fig. 1(a)], respectively, were still present in Figure 1(b), indicating that the long range order of SBA-15 was not destroyed after the encapsulation of polypyrrole (PPY) into SBA-15. However, the decrease of intensity and the increase of the  $2\theta$  of all of the three peaks in Figure 1(b) confirmed the encapsulation of

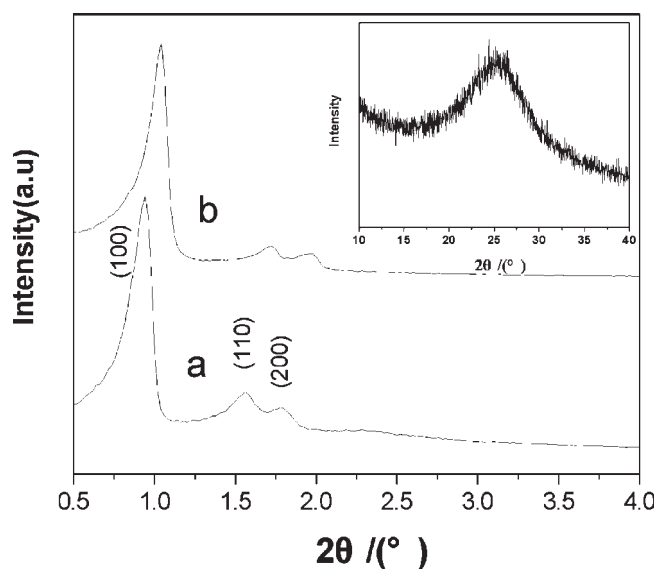


**Figure 1** The lower angle XRD patterns of (a) SBA-15, (b) PPY/SBA-15, and inset in Figure 1 was the wide angle XRD pattern of PPY.

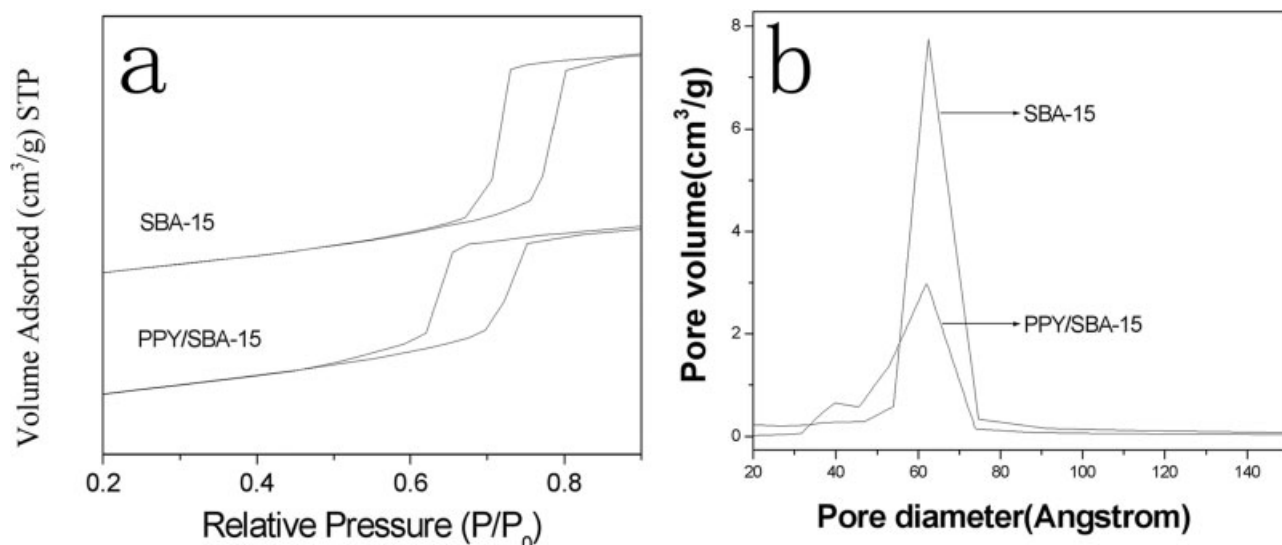
PPY into SBA-15. The inset in Figure 1 was the wide angle XRD pattern of PPY, which showed a broad feature centered at  $2\theta = 25.0^\circ$ , which can be assigned to the interchain spacing of PPY.<sup>13</sup>

### $\text{N}_2$ adsorption–desorption characterization

To prove the encapsulation of PPY into SBA-15 further, we showed the  $\text{N}_2$  adsorption–desorption isotherms and pore size distribution curves of SBA-15 and PPY/SBA-15 in Figure 2. As can be seen from Figure 2(a), both traces were of Type IV, suggesting the typical form of mesoporous materials. For the curve of PPY/SBA-15, the inflection of the step shifted to a smaller  $P/P_0$ , indicating that the pore size of SBA-15 become smaller after the inclusion of PPY into SBA-15. The pore size distributions, calculated from the desorption isotherms, were shown in Figure 2(b). As can be seen from Figure 2(b), the centered pore size changed from 6.25 nm for pure SBA-15 to 3.97 nm for PPY/SBA-15. At the same time, it could be observed that there was also a peak centered at 6.21 nm for PPY/SBA-15, indicating that some pores of SBA-15 were not filled with PPY. In addition, the BET surface area varied from  $591.86 \text{ m}^2 \text{ g}^{-1}$  for SBA-15 to  $268.40 \text{ m}^2 \text{ g}^{-1}$  for PPY/SBA-15, and the pore volume decreases from  $0.8916 \text{ cm}^3 \text{ g}^{-1}$  (SBA-15) to  $0.50340 \text{ cm}^3 \text{ g}^{-1}$  (PPY/SBA-15). All these results confirmed the successful encapsulation of PPY into SBA-15.

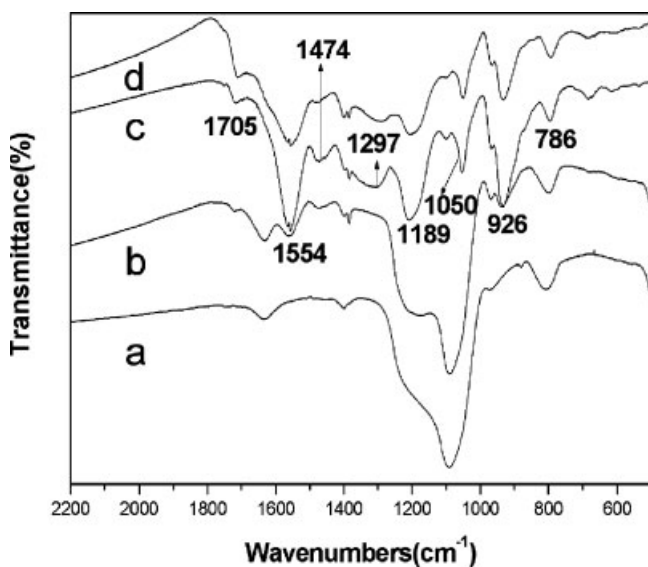
### IR spectroscopy

Figure 3 shows the infrared spectra of (a) SBA-15, (b) PPY/SBA-15 composites, (c) pure PPY, and (d) PPY/SBA-15 after removing SBA-15 with fluoride acid (HF)



**Figure 2** Nitrogen adsorption-desorption isotherms (a) and the pore size distribution curves (b) of SBA-15 and PPY/SBA-15.

for 24 h. In the curve c of Figure 3, the peak at  $786\text{ cm}^{-1}$  is characteristic of the C—H out-of-plane bending model. The band assigned to the C—H in-plane deformation vibration of pyrrole ring appears at  $1050\text{ cm}^{-1}$ .<sup>13</sup> The bands observed at  $1474$  and  $1189\text{ cm}^{-1}$  represent the C—N stretching vibration, this is agreement with that in literature.<sup>14</sup> The peak appears at  $1554\text{ cm}^{-1}$  comes from the C—C stretching vibration. The weak band around  $1705\text{ cm}^{-1}$  is normally attributed to the C—O stretching, which suggests that the pyrrole rings were slightly overoxidized.<sup>13,14</sup> According to Weixin Zhang et al., the C—O groups were present in chemically synthesized PPY, and some of the oxidized pyrrole rings, such as pyrrolidone formed



**Figure 3** IR spectrum of (a) SBA-15, (b) PPY/SBA-15 composites, (c) pure PPY, and (d) PPY/SBA-15 after removing SBA-15 with HF for 24 h.

during the growth process. The bands at  $1297$  and  $926\text{ cm}^{-1}$  may be assigned to the doped bands. According to Kityk group's work,<sup>15</sup> in which they investigated the nonlinear optical properties of the Ru-doped PMMA guest host composite materials, there may appear the effects of electron-vibration anharmonic interactions due to the electrostatic potential gradients on the borders. These electron-vibration anharmonic interactions are related to the charge density non-centrosymmetry which determines the efficiency of the humidity. In addition, as can be seen from Figure 3, the characteristic peaks at  $1050$ ,  $1189$ , and  $1297\text{ cm}^{-1}$  been assigned to PPY disappear completely and the intensity of the peaks at  $926$ ,  $1474$ , and  $1554\text{ cm}^{-1}$  decrease in the spectra of PPY/SBA-15, as given in Figures 3(b) and 3(c). The phenomenon demonstrates that most part of PPY have been encapsulated into the pores of SBA-15. To confirm this conclusion, the sample of PPY/SBA-15 was treated with HF for 24 h, then washed three times with distilled water and dried at room temperature. As shown in Figure 3(d), all the characteristic peaks attributed to PPY appear again and return to the normal intensity.

#### Humidity sensitive properties

The humidity sensitive properties (HSP) of PPY and PPY/SBA-15 were studied using a ZL-5 model LCR analyzer at room temperature,  $1\text{ kHz}$ , and  $1.0\text{ V}$ . As shown in Figure 4, for the pure PPY [Fig. 4(a)], the variation range of impedance is less significant when the relative humidity changes from  $11\%$  to  $95\% \text{ RH}$ . However, after encapsulation of PPY into SBA-15 [Fig. 4(c)], the impedance varies from  $3.7 \times 10^6\ \Omega$  ( $11\% \text{ RH}$ ) to  $2.0 \times 10^4\ \Omega$  ( $95\% \text{ RH}$ ). Namely, the impedance of PPY/SBA-15 decreases by two to three orders of mag-

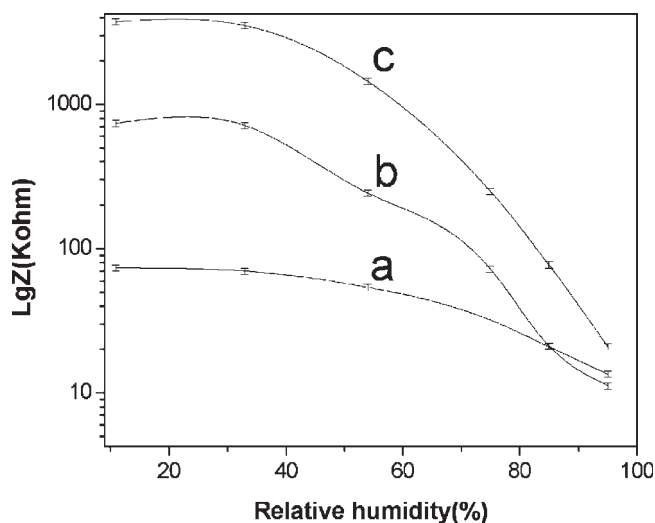
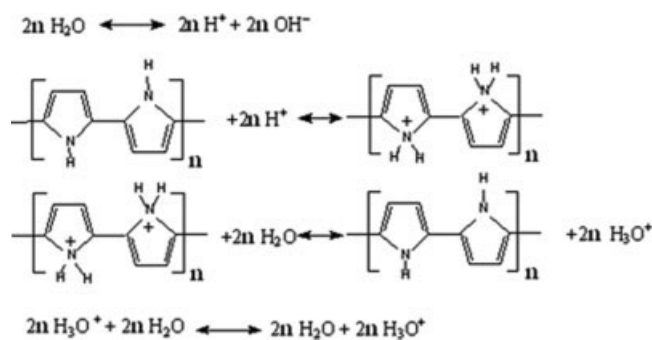


**Figure 4** Humidity sensitive property curves of (a) pure PPY, (b) SBA-15, and (c) PPY/SBA-15.

nitude when the relative humidity changes from 11% RH to 95% RH, showing higher sensitivity than that of the pure PPY. In addition, we give the HSP curve of pure SBA-15 [Fig. 4(b)] for reference. As can be seen from Figure 4, the impedance of pure SBA-15 is between that of pure PPY and PPY/SBA-15 at the same relative humidity, and its variation is nonlinear at higher relative humidity. Here, we try to give a mechanism to explain why the PPY/SBA-15 composites exhibit higher HSP than that of the corresponding pure PPY.

The main conductive method of PPY and PPY/SBA-15 in presence of water is considered to be the proton exchange mechanism<sup>16</sup> between PPY and the adsorbed water. The transfer process of proton in the system of PPY and PPY/SBA-15 can be explained in a simple form as shown in Scheme 1.



**Scheme 1** The transfer process of proton in the system of PPY and PPY/SBA-15.

For the pure PPY, it has a morphology of micro-sized particles [Fig. 5(a)], the particle size is about 200–500 nm. When the electrode coated with pure PPY was placed into the bottle filled with moisture, the adsorbed water content became saturated quickly, because that water molecular can be easily adsorbed onto the PPY around the micro-sized particles, as shown in Scheme 2(a). The arrowhead direction represent the direction from which water molecule was adsorbed. The saturated adsorbed water improves the conductivity of PPY, so its impedance is lower and shows lower sensitivity when the RH ranges from 11% to 95%. However, when the PPY was encapsulated into SBA-15, it obtained morphology of bunch of rods, as shown in Figure 5(b). At lower humidity, due to the isolated effect of SBA-15, water molecules entered into the pores of SBA-15 only through the two ends of the pores of SBA-15, as shown in Scheme 2(b). In this process, water molecules could not form continuous water layer, the transfer of  $\text{H}^+$  or  $\text{H}_3\text{O}^+$  is so difficult on the discontinuous water layer that PPY/SBA-15 exhibit high impedance at lower humidity. As the relative humidity increased, one or several serial water layers

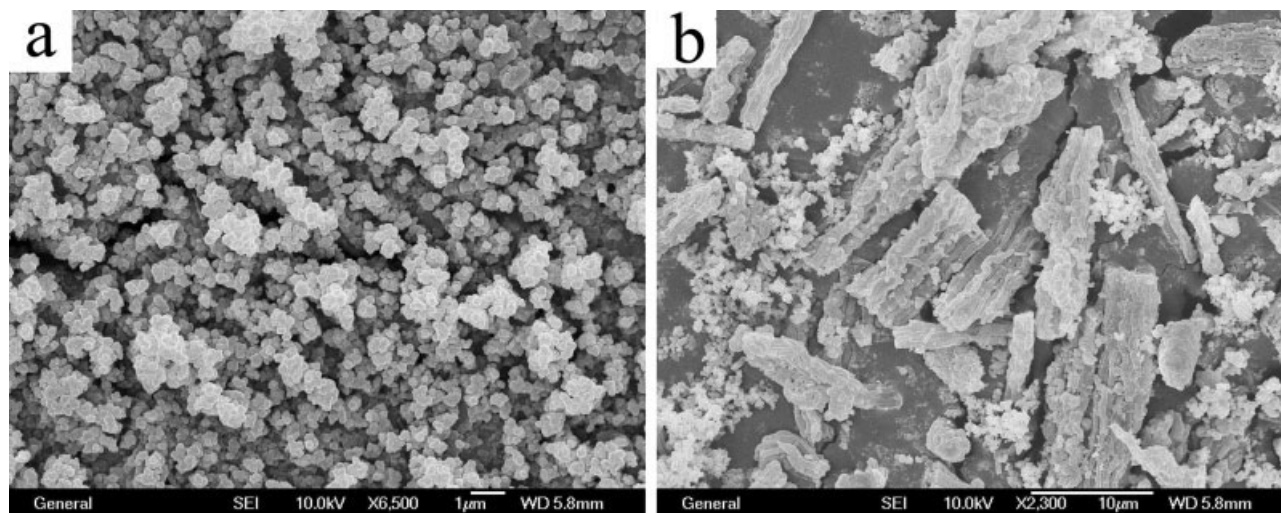
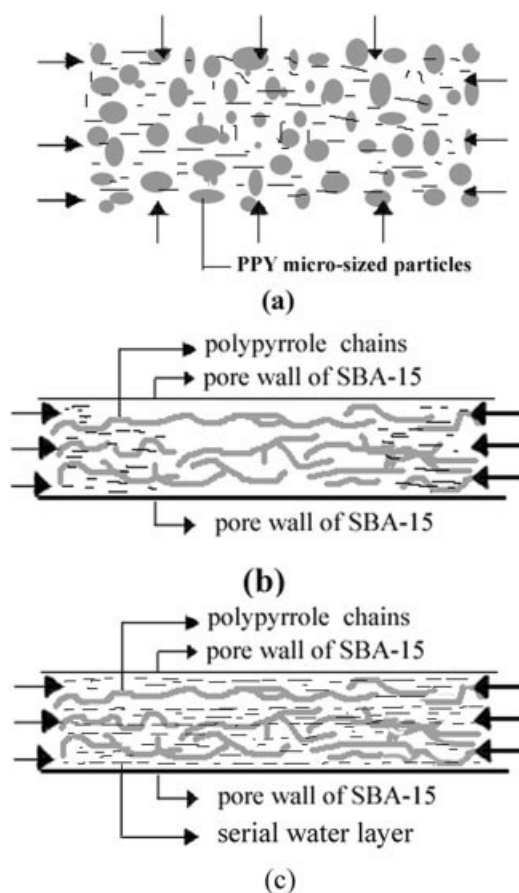


**Figure 5** SEM image of (a) PPY and (b) PPY/SBA-15.



**Scheme 2** Illustration of the adsorption process of water in (a) PPY, (b) PPY/SBA-15 at lower relative humidity, and (c) PPY/SBA-15 at higher relative humidity. The dashed line represent water molecule, the direction of that water molecule was adsorbed was pointed by arrowheads.

were formed between the pore walls and the surface of PPY chains, or between two PPY chains [Scheme 2(c)]. The serial water layers accelerated the transfer of  $H^+$  or  $H_3O^+$ . According to the ion transfer mechanism of Grotthuss,<sup>17</sup>  $H_2O + H_3O^+ = H_3O^+ + H_2O$ , the initial state and final state are same, the energy is also equivalent, so the transfer of ion is quite easy. The quick transfer of ion on the water layer result in the sharply decrease of the impedance. So the PPY/SBA-15 host-guest composite materials show higher humidity sensitive properties than the corresponding pure PPY.

## CONCLUSIONS

PPY and PPY/SBA-15 host-guest composite materials have been successfully synthesized. The characterization of XRD, IR spectra, and  $N_2$  adsorption-desorption isotherms shows the formation of PPY and the successful encapsulation of PPY into SBA-15. The morphology of PPY and PPY/SBA-15 was obtained by SEM. The studies of HSP indicated that PPY encapsulated into SBA-15 behaves higher humidity sensitivity. We think that serial adsorbed water layers play an important role in the improvement of the humidity sensitivity properties of PPY/SBA-15 host-guest composite materials.

The authors acknowledge Dr. Xiaojun Yin for generous help in SEM, and we are grateful to Dr. Tong Zhang for her timely help in the field of humidity sensors.

## References

- Kang, J.; Park, S. *Mechatronics* 1998, 8, 459.
- Park, S.; Kang, J.; Park, J.; Mun, S. *Sens Actuators B* 2001, 76, 322.
- Connolly, E. J.; Pham, H. T. M.; Groeneweg, J. *Sens Actuators B* 2004, 100, 216.
- Hassen, M. A.; Clarke, A. G.; Swetnam, M. A.; Kumar, R. V.; Fray, D. J. *Sens Actuators B* 2000, 69, 138.
- Li, Y.; Yang, M. J.; She, Y. *Talanta* 2004, 62, 707.
- Li, N.; Li, X. T.; Geng, W. C.; Zhang, T.; Zuo, Y.; Qiu, S. L. *J Appl Polym Sci* 2004, 93, 1597.
- Hsu, S. C.; Lee, C. F.; Chiu, W. Y. *J Appl Polym Sci* 1999, 71, 47.
- Wu, S. Z.; Zhu, Y. L.; Li, F. X.; Shen, J. R. *J Appl Polym Sci* 1999, 74, 1992.
- Li, Y.; Yang, M. J. *Sens Actuators B* 2002, 86, 155.
- Li, Y.; Yang, M. J. *Sens Actuators B* 2002, 85, 73.
- Zhao, D.; Feng, J.; Huo, Q.; Melosh, N.; Fredrickson, G. H.; Chmelka, B. F.; Stucky, G. D. *Science* 1998, 279, 548.
- Zhao, D.; Huo, Q.; Feng, J.; Chmelka, B. F.; Stucky, G. D. *J Am Chem Soc* 1998, 120, 6024.
- Zhang, W. X.; Wen, X. G.; Yang, S. H. *Langmuir* 2003, 19, 4420.
- Qu, L. T.; Shi, G. Q. *Macromolecules* 2003, 36, 1063.
- Migalska-Zalas, A.; Sofiani, Z.; Sahraoui, B.; Kityk, I. V.; Tkaczyk, S.; Yuvshenko, V.; Fillaut, J. L.; Perruchon, J.; Muller, T. J. J. *J Phys Chem B* 2004, 108, 14942.
- Jain, S.; Chakane, S.; Samui, A. B.; Krishnamurthy, V. N.; Bhoraskar, S. V. *Sens Actuators B* 2003, 96, 124.
- Ernsberger, F. M. *J Am Ceram Soc* 1983, 11, 747.